NUMERICAL MODELLING OF STRESS STATE AND DEFORMATIONS IN LASER BUTT-WELDED SHEETS MADE OF X5CRNI18-10 STEEL

PIEKARSKA Wiesława, SATERNUS Zbigniew, KUBIAK Marcin, DOMAŃSKI Tomasz

Czestochowa University of Technology, Institute of Mechanics and Machine Design Foundations, Czestochowa, Poland, EU, piekarska@imipkm.pcz.pl

Abstract

This work concerns numerical simulations of thermomechanical phenomena in laser butt-welding of sheets made of X5CrNi18-10 steel. Abaqus FEA software is used in calculations taking into account phase transformations during material's state changes and temperature dependent thermomechanical properties of analysed steel. Additional numerical subroutines are implemented into Abaqus solver in order to describe the movable heat source power intensity distribution.
The shape and size of melted zone is predicted as well as residual stress and deformations. Real butt-welded joints are executed in order to verify the results of numerical simulations. Numerically predicted deflection of the joint is compared to real displacement, measured using profile-graphometer New Form Talysurf 2D/3D 120. Melted zone of the cross section of the joint is compared to numerically predicted geometry of the fusion zone.

Keywords: Laser welding, Welding deformations, Residual stress, Numerical modelling, Abaqus FEA

1. INTRODUCTION

Highly concentrated heat source used in laser beam welding process causes rapid material melting which allow achieving the high welding speed and narrow melted zone. A local increase in temperature leads not only to melting but also to the partial evaporation of steel and to formation of the melting pool as well as keyhole [1]. The keyhole also stands for the heat source penetrating material. In this welding technique a good quality welds are obtained with a narrow thermal influence zone, which is helpful in reducing deformations and residual stress in the work piece and helpful in increasing quality and efficiency of production process [2]. This is particularly important in welding of long constructions.

Deformations occurring during welding are one of the major problems in the design of welded constructions. The character and size of deformations depends on the physical properties of the material, rigidity of a construction and the welding method. The proper selection of the welding technology can reduce deformations in a large extent. Unquestionable advantages of laser welding contribute to the very intense development of this technology and wide application in the industry. However, the proper use of this joining method requires a quantitative analysis and control of occurring deformations and residual stress in welded joints for assumed various process parameters. At the time the computer simulations by mathematical and numerical modelling of physical phenomena occurring in the process becomes a helpful tool [3-7].

This work concerns numerical modelling of thermomechanical phenomena in laser welding process, performed to predict distortion and residual stress in butt-welded sheets made of X5CrNi18-10 steel. Computer simulations of temperature field as well as stress and strain states are performed in Abaqus FEA supplemented by additional subroutines where movable heat source power distribution is implemented. Presented results include temperature distribution, residual stress and the comparison of predicted fusion zone with the macroscopic picture of the real butt-welded joint cross-section as well as the comparison of estimated deflections and real displacement, measured using profile-graphometer New Form Talysurf 2D/3D 120.

2. NUMERICAL MODELING

Thermal and mechanical phenomena in welded joints are determined using Abaqus FEA, engineering software. Analysed system with marked boundary conditions used in mechanical analysis is presented in **Fig. 1**.

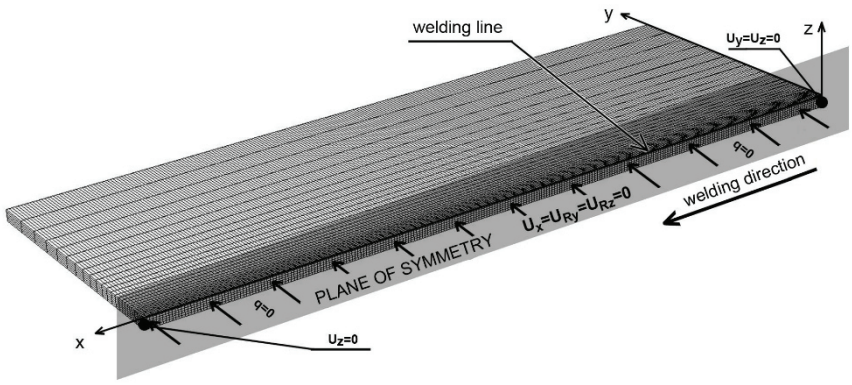

Fig. 1 Scheme of analyzed domain. Discrete model with boundary conditions

The analysis of thermal phenomena is made on the basis of the solution of energy conservation equation together with Fourier law [8]. Temperature field expressed in the criterion of weighted residuals method is described by the following equation:

$$\int_V \rho \frac{\partial U}{\partial t} \delta T \, dV + \int_V \frac{\partial \delta T}{\partial x_\alpha} \cdot \left(\lambda \frac{\partial T}{\partial x_\alpha} \right) dV = \int_V \delta T \, q_V \, dV + \int_S \delta T \, q_S \, dS \tag{1}$$

where $\lambda=\lambda(T)$ is a thermal conductivity [W/(m K)], $U = U(T)$ is a internal energy, q_v is laser beam heat source [W/m^3], q_S is a heat flux toward elements surface [W/m^2], δT is a variational function, ρ is a density [kg/m^3].

Equation (1) is completed by initial condition $t = 0 : T = T_o$ and boundary conditions of Dirichlet, Neumann and Newton type taking into account heat loss due to convection and radiation as well as welding heat flux towards heated surface. Effective convection-radiation coefficient is assumed in calculations [4] and constant ambient temperature $T_0 = 20$ °C. On the surface of laser beam impact, heat dissipation is forced due to the liquid material flow in the fusion zone and blow of shielding gas. Therefore, model proposed by Mundra and DebRoy [5] is used in the analysis. On remaining boundaries of the T-joint Vinokurov model [6] is assumed for constant radiation coefficient ($\varepsilon = 0.5$).

Fuzzy solidification front is assumed in the model [4, 5, 7]. Internal energy U in equation (1) takes into account the latent heat of fusion $H_L=260\times10^3$ J/kg in the mushy zone (between solidus temperature T_S=1400°C and liquidus temperature T_L=1450 °C).

The analysis of temperature field is performed in Lagrange coordinates, hence heat transfer equation (1) is considered without convection unit. Coordinates of the centre of welding heat source is determined for each time step in additional subroutine DFLUX, implemented in Fortran programming language. Implemented model takes into account assumed welding speed. Welding heat source is described by Gaussian distribution along radial direction with linear decrease of energy density along material penetration depth [5], expressed as follows:

$$q_v(r,z) = \frac{3 \cdot Q}{\pi r_o^2 s} \exp\left[\left(1 - \frac{r^2}{r_o^2} \right) \right] \left(1 - \frac{z}{s} \right) \tag{2}$$

where Q is laser beam power [W], r_0 is beam radius [m], $r=\sqrt{x^2+y^2}$ is actual radius [m], s is penetration depth [m], z is an actual penetration [m].

Mechanical analysis in elastic-plastic range is based on classic equilibrium equations, supplemented by constitutive relations as well as initial and boundary conditions (**Fig. 1**), which are assumed to ensure the external static determination of considered system [9]:

$$\nabla \circ \dot{\boldsymbol{\sigma}}(x_\alpha,t)=0, \qquad \dot{\boldsymbol{\sigma}}=\dot{\boldsymbol{\sigma}}^T \tag{3}$$

$$\dot{\boldsymbol{\sigma}}=\mathbf{D}\circ\dot{\boldsymbol{\varepsilon}}^e+\dot{\mathbf{D}}\circ\boldsymbol{\varepsilon}^e \tag{4}$$

$$\boldsymbol{\sigma}(x_\alpha,t_0)=\boldsymbol{\sigma}(x_\alpha,T_S)=0, \qquad \boldsymbol{\varepsilon}^e(x_\alpha,t_0)=\boldsymbol{\varepsilon}^e(x_\alpha,T_S)=0 \tag{5}$$

where $\boldsymbol{\sigma}=\boldsymbol{\sigma}(\sigma_{ij})$ is stress tensor, x_α describes location of considered point (material particle), ($\circ$) is inner exhaustive product, $\mathbf{D}=\mathbf{D}(T)$ is a tensor of temperature dependent material properties, presented in **Table 1**.

Elastic strain is modelled for isotropic material using Hooke's law with temperature depended Young's modulus and Poisson's ratio. Plastic flow model is used to determine plastic strain based on Huber-Mises yield criterion and isotropic strengthening.

Table 1 Assumed thermomechanical properties of X5CrNi18-10 steel [7]

Thermal properties				Mechanical properties				
T [°C]	λ [W/m °C]	ρ [kg/m³]	c [J/kg °C]	T [°C]	E [GPa]	Re [MPa]	v [-]	α^T [1/°C]
0	14.6	7900	462	0	198,5	265	0.294	1.7 e-5
100	15.1	7880	496	100	193	218	0.295	1.74 e-5
200	16.1	7830	512	200	185	186	0.301	1.8 e-5
300	17.9	7790	525	300	176	170	0.31	1.86 e-5
400	18	7750	540	400	167	155	0.318	1.91 e-5
600	20.8	7660	577	600	159	149	0.326	1.96 e-5
800	23.9	7560	604	800	151	91	0.333	2.02 e-5
1200	32.2	7370	676	1200	60	25	0.339	2.07 e-5
1300	33.7	7320	692	1300	20	21	0,342	2.11 e-5
1600	120	7320	700	1600	10	10	0.388	2.16 e-5

T - temperature; *λ*- conductivity; *ρ*- density; *c* - specific heat;
E - Young modulus; *Re* - yield stress; *v* - Poisson ratio; α^T - thermal expansion coefficient

3. RESULTS AND DISCUSSION

Laser butt-welding process is performed at Welding Institute in Gliwice on robotic welding station equipped with Trumpf TruDisk 12002 laser having maximum power 12 kW. The joint consisting of two plates made of steel type 304 (X5CrNi18-10) is made without additional material and without a gap.

The displacement of laser butt-welded joints is measured using laboratory New Form Talysurf profilographometer 2D/3D Taylor Hobson 120. Measurement scheme of the displacement along z-axis in perpendicular direction to the weld line (the deflection) is shown in **Fig. 2**.

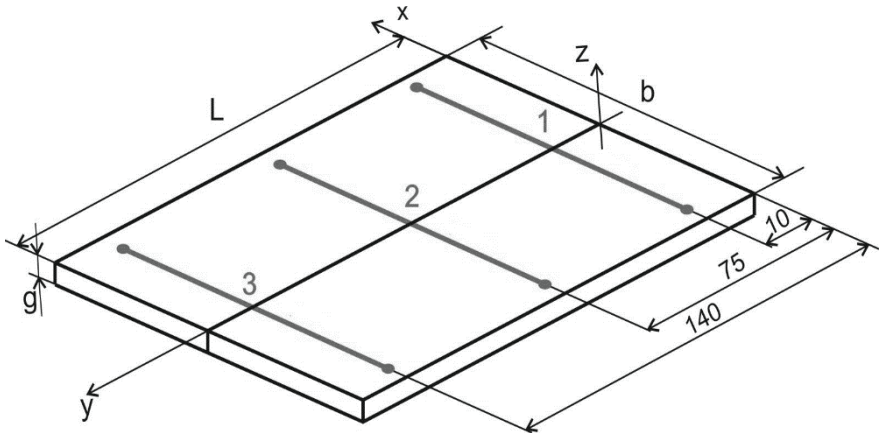

Fig. 2 Measurements of deformations scheme (L = 150 mm, L_p = 60 mm, b = 90 mm, g = 2 mm

The same process parameters are used in all numerical simulations as in experimental research. Laser beam power Q = 3 kW, beam radius r_0 = 0.3 mm, and welding speed v = 5.2 m/min. Heat source penetration depth is assumed as s = 0.6 mm on the basis of experimental verification. In order to reduce computational time, symmetry of the joint is assumed in calculations taking into account appropriate boundary conditions in the plane of symmetry (**Fig. 1**).

Obtained temperature distribution in the longitudinal section and cross section of welded joint is presented in **Fig. 3** where solid line points out the boundary of melted zone (isoline $T_L \approx 1450^{o}$C). Additionally, in this figure the comparison between numerically estimated characteristic zones in the cross section of the joint and the real weld is presented.

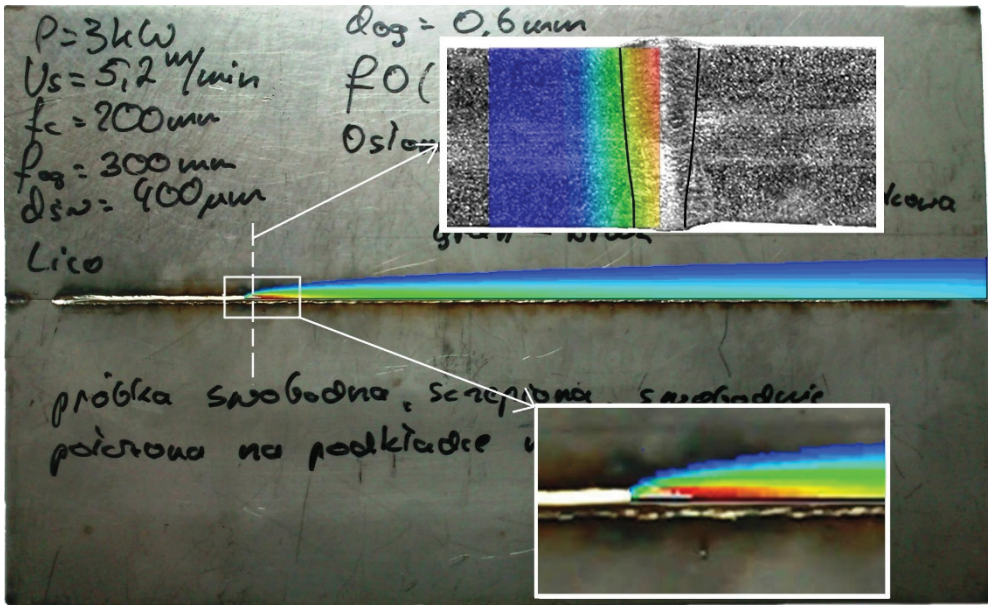

Fig. 3 Temperature distribution in welded joint with the comparison of predicted melted zone and the real weld cross-section

Numerically estimated displacement u_z along x-axis in laser welded joint is illustrated in **Fig. 4** for three chosen lines that correspond to experimentally measured deflection along lines presented in **Fig. 2**. Distributions of longitudinal reduced residual stresses at the edge and central fibers (lines 1 and 2) and at upper layers (from the face of the weld) and lower layers (from the ridge of the weld) are shown in **Fig. 5**.

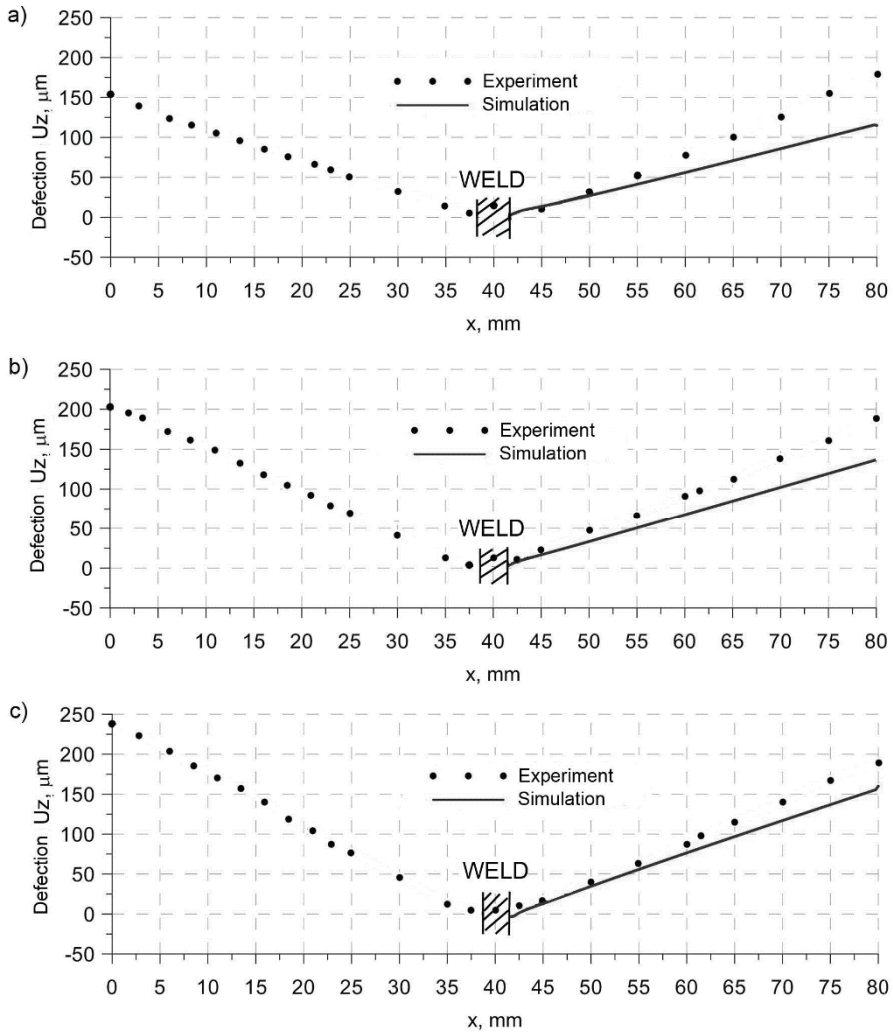

Fig. 4 Deflection along x-axis: a) line 1, b) line 2, c) line 3 (corresponding to **Fig. 2**)

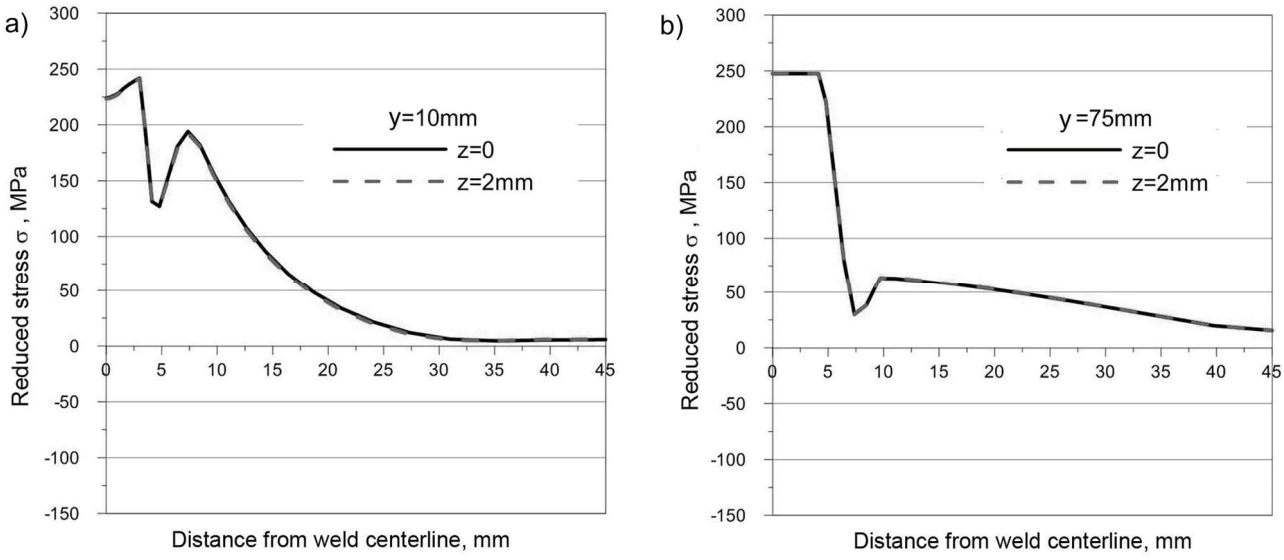

Fig. 5 Residual reduced stress σ

CONCLUSIONS

The comparison of weld geometry and predicted melted zone shape (**Fig. 3**) and the comparison of estimated deflection with the real displacement in welded joint (**Fig. 4**) shows a good agreement of results of numerical analysis with the experiment which indicates the correctness of developed mathematical and numerical models of thermal and mechanical phenomena in the laser beam welding process.

Numerical analysis and experimental research confirmed that laser welded joint is deformed in the transverse and longitudinal directions to the weld line. This is also confirmed by stress distributions. Obtained residual stress reaches maximum values ~250 MPa in the weld (**Fig. 5**). Deflection is small and reaches highest value in welded sheets below 250 μm (**Fig. 4**).

Presented models of the analysis of thermomechanical phenomena in Abaqus FEA software, allows for the comprehensive analysis of welding process, including welding deformations in terms of different process parameters. Therefore developed model may be useful for selecting appropriate parameters that allow obtaining the proper geometry, quality and mechanical properties the designed joint.

REFERENCES

[1] DAWES, C. Laser Welding, Abington Publishing, New York, 1992.

[2] PILARCZYK, J., BANASIK, M., DWORAK, J., STANO S. Technological applications of laser beam welding and cutting at the Instytut Spawalnictwa. Przeglad Spawalnictwa, Vol. 5-6, 2006, pp. 6-10.

[3] DENG D., MURAKAWA H. Prediction of welding distortion and residual stress in a thin plate butt-welded joint. Computational Materials Science, Vol. 43, 2008, pp. 353-365.

[4] DENG D., FEM prediction of welding residual stress and distortion in carbon steel considering phase transformation effect. Materials and Design, Vol. 30, 2009, pp. 359-366.

[5] BOKOTA A., PIEKARSKA W. Modeling of residual stresses in laser welding. Paton Welding Journal, Vol. 6, 2008, pp. 19-25.

[6] LACKI P., KUCHARCZYK Z., ŚLIWA R.E., GAŁACZYŃSKI T. Effect of Tool Shape on Temperature Field in Friction Stir Spot Welding. Archives of Metallurgy and Materials, Vol. 58, 2013, pp. 597-601.

[7] PIEKARSKA, W., KUBIAK, M., SATERNUS Z., REK K. Computer modelling of thermomechanical phenomena in pipes welded using a laser beam. Archives of Metallurgy and Materials, Vol. 58, 2013, pp. 1237-1242.

[8] DASSAULT SYSTEM, Abaqus theory manual. Version 6.7, SIMULIA, 2007.

[9] BOKOTA, A., DOMAŃSKI, T. Numerical analysis of thermo-mechanical phenomena of hardening process of elements made of carbon steel C80U. Archives of Metallurgy and Materials, Vol. 52, 2007, pp. 277-288.